Numerical Modeling of the tridimensional responses of induction logging in the occurrence of different geometries of invasion zones

Alfredo Carrasco & Abel Carrasquilla, UENF/CCT/LENEP – Macaé, RJ

Abstract

The electromagnetic induction logging is one of the wellbore geophysical techniques frequently used to known the resistivity of the reservoir virgin zone, because of the high investigation depth. But this resistivity response can be modified by the mud filtrate entering into the formation during the well drilling process. So, the objective of this work is to obtain the well logging responses of the well induction when exists different tridimensional geometries of invasion zones, using an algorithm based on the integral equation method. The well tool used in this simulation was the classic 6FF40 from the SCHLUMBERGER, which results show the effects of the invasion zone in the well logging responses, for the ramp and slope model, and significantly more influenced when annulus is present.

Introduction

The geophysical well logging is an important tool in hydrocarbon exploration, mainly in the petrophysics characterization of the reservoir, since it is a technique that represents a small percentage of the well cost, and provides important information of the rock. Among the well logging tools, the electromagnetic induction, developed in the forties years, is used for measuring the resistivity formation when non conductivity mud (oil based) is present. In that sense, a resistivity measurement of the virgin zone (Rt) is a very important parameter for knowing the potential production of the formation and its oil saturation, using the Archie law (Dewan, 1983).

During the drilling process exists an invasion of the liquid part from the mud drilling to the permeate zones, since hydrostatic pressure is greater than formation. This causes a displacement of the original fluids in an irregular way and its depth into the formation depends on its lithology and petrophysical characteristics. So, it is necessary to understand the effect of the invasion zone on the well induction log responses by using numerical simulation (Anderson, 2001).

Methodology

In this study is used a focused array tool called 6FF40 from the SCHLUMBERGER (Anderson, 2001) and a numerical technique of integral equations in order to simulate different types of tridimensional invasion (3D). This numerical concept involves the resolution of the primary field of the surroundings of the 3D body in the one-dimensional (1D) stratified bedding. Then, the heterogeneous body 3D is discretized in a set of prisms (Hohmann, 1975). The formulation of this technique in physics problems have to prove being more efficient and compact than differential equations, because the boundary conditions are considered automatically into their formulation. Given the possibility to get the heterogeneity discretized, this scope uses less memory capacity and therefore, less computational time. For this reason, it is considered the best method for solving 3D electromagnetic problems, specially when the heterogeneity bodies are small (Carrasquilla, 1993).

In fact, little is known about the real geometry of invasion and there is no satisfactory method for its measuring in situ. A very used simplified method for obtaining Rt is the piston model. This model can be described as an uniform displacement of the originals fluids into the permeable formation by the liquid part of the mud drilling (flushed zone with resistivity Rxo). For reservoirs without water drive and gas cap, we can use the ramp and slope model (Figure 1 and 2) as defined by Singer and Barber (1988), All these models consider a bedding sequence of shale – reservoir formation – shale with resistivities of 1 ohm-m, 100 ohm-m and 1 ohm-m, respectively. A reservoir formation between the shale contents oil.

In the figure 1 we can observe a transition zone instead of a flushing zone, and its extension will depend on some petrophysical parameters, as porosity, permeability, capillary pressure and density of the invasor fluid, among others. In this model is observed a linear changing of the transition zone from the wellbore to virgin zone, and this is the first model to be simulated in this work.

In the slop model (figure 2), there is a linear transition from the wellbore in the flushed zone, to the virgin zone. This is our second model to be simulated.

Finally, we simulate a reservoir with water drive using a model invasion when annulus is present. Singer and Barber (1988) defines this zone as typical in reservoirs with hydrocarbons mobility is greater than water. In this case, there is a zone formed where hydrocarbon is displaced by water formation. In the figure 3, we can see an annulus created in the lower part and its representation considering the resistivity values. This is the third model to be simulated in this work (Figure 4).

In the ramp model are considered prismatic cells of 0,2 m length and 0,4 m height. The wellbore diameter was defined with cells of 0,2 m, making a total diameter of 7,9 inches.

Figure 5 shows a schematic vision of the half part of the ramp model, with an upper image (Figure 5a) and a transversal section in Figure 5b. A resistivity inside the wellbore is 1 ohm-m represented by cells with number 1. The shaded region is the flushed zone, with a 0,7m of depth extension, represented by cells numbered with 2 and 3, and with resistivity values of 20 and 50 ohm-m, respectively. The zone 3 resistivity was defined as a intermediate resistivity between the flushed and virgin zone (35 ohm-m). The virgin zone resistivity is mark with the 4 number and has 100 ohm.m of resistivity (Semmelbeck & Holditch, 1988).

In the slope model invasion, we use the same geometry of the ramp model, if we consider the dimensions and the resistivity values. The difference is present in the superior part of the model (Figure 6). Experiences made by Gondouin and Heim (1964) in aquifer sands, shows that the invasion ramp format appears in small invasions and invasion slope format comes out in strong invasions. Once more we considered an intermediate zone located between the flushed and virgin zone mark as number 3 and with 35 ohm-m of resistivity. It is believed that this transition zone was created by events as mud fingering into a region next to the virgin zone (Jiao & Sharma, 1991).

In the annulus model is important to consider the formation water resistivity lower the mud filtrate resistivity, as was observed experimentally by Jiao and Sharma (1991), because when values of Rmf and Rw resistivities are equal, there is no annulus formed. In this case, the annulus is created when the mud cake is still absent and the rate of invasion is high, and consequently, the most part of the oil is displaced to the upper part in a short period of time and simultaneously occurs a miscible displacement of the original brine by the higher resistivity of the mud filter (Figure 4). The result from these two situations is the annulus generation; witch is characterized for having low values of resistivity and has a strong influence in the induction responses (Singer & Barber, 1988). In that sense, the resistivity and depth investigation parameters for the annulus model were obtained from the work of Bovan et al (2003), as shown in the Figure 7. A distribution of resistivities represents a general scheme of a oil reservoir above an aquifer. The configuration of this model are the following: wellbore diameter of 7,9 inches with contains drilling fluid of 1 ohm.m of resistivity (indicated by cells numbered in 1), a flushed zone with 20 ohm-m of resistivity (cells number 2) at a radial distance of 0,7m; a annulus region with 0,1 ohm-m of resistivity (pointed cells) and 0,4 m width, and the oil reservoir virgin zone with 100 ohm-m of resistivity (cells number 4).

Results

The response of the 6FF40 tool for the 3D invasion ramp model (Figure 5) appears in a red trace in figure 8. The blue straight lines represent the 1D resistivities distribution without considering the 3D heterogeneity body. For comparison, the same sequence of resistivity for the 3D model was included for the 3D model without considering the fluid entering into the formation, as indicated by green traced in the picture. So, we can observe that invasion causes a little diminution on the resistivities values in the lower part of the curve, because of the model used.

In the case of the slope model of the figure 6, the resistivities values were maintained, as well as cells dimensions, changing only the geometry of the zone invasion. As well as the ramp model, there is also a diminution in the resistivities values in the lower part of the red curve, with similar responses (Figure 9). Also in this case, we show the resistivity curve 1D in blue, and a 3D response without invasion in green color.

Finally, for the model corresponding to the figure 7, we can note a strong influence from the annulus, in most of the extension of the resistivity red curve, with resistivities values lower than those obtained using the ramp and slope model (Figure 10). To make this model, it was considered an aquifer with 2 ohm-m of resistivity and 0,8 meters of thickness. As shown in the last cases, we show the resistivity responses 1D in blue color and the response without considering the 3D invasion in green color.

Conclusions

The results obtained in the numerical simulation of the electromagnetic well logging induction responses, when a invasion is present and represented with a 3D geometry and solved using an integral equation algorithm shows a modification in the induction responses, as shown in the ramp and slop model cases. This effect is strong when annulus is present. In this case, a 6FF40 tool is very sensible to the lower resistivity of the annulus, and can generate lower estimations in the reserve calculations. This lower resistivity is related to the salinity water formation and that of the mud filter, and consequently the geometric characteristics of the annulus are depending on the reservoir petrophysical parameters.

Acknowledgments

To the North Fluminense State University Darcy Ribeiro (UENF) by the computational support, to the Society of Petroleum Engineering (SPE) by the accessibility to the papers for consulting and to the CARMOD net by the financial support of the project.

References

Anderson, B. 2001. Modeling and inversion methods for the interpretation of resistivity logging tool response. PhD Thesis, DUP Science, Delft, The Netherlands, 386 p.

Bovan, G.; Torres-Verdín, C.; Delshad, M; Sigal, R.; Zouioueche, F. & Anderson, B. 2003. A case study integrating the physics of mud-filtrate invasion with the physics of induction logging: assessment of in-situ hydrocarbon saturation in the presence of deep invasion and highly saline connate water. Research Report, University of Texas, 14 p.

Carrasquilla A. 1993. Modelagem numérica da influência do eletrojato equatorial em dados magnetotelúricos produzidos por estruturas tridimensionais. Tese de Doutorado, Universidade Federal do Pará, Belém, 176p.

Dewan, J. 1983. Essentials of Modern Open-Hole Log Interpretation. PennWell Publishing Company, Tulsa, OK, 361 pp.

Gondouin, M., Heim, A. 1964. Experimentally determined resistivity profiles in invaded water and oil sands for linear flows. Journal of Petroleum Technology, Volume 16, Number 3, p. 337-348

Hohmann, G. W. 1975. Three-dimensional induced polarization and electromagnetic modeling. Geophysics, 40:309-324.

Jiao, D. & Sharma, M. 1992. An experimental investigation of the resistivity profile in the flushed zone. The Log Analyst, SPWLA, Vol. 33, No. 2, 10 pp.

Singer, J. & Barber, T. 1988. The effect of transition zones on the response of induction logs, SPWLA Symposium, 29th, San Antonio, Tex., 1988, Transactions, p. L1-L13.

Semmelbeck, M. & Holditch S. 1988. The effects of mud filtrate invasion on the interpretation of induction logs. SPE Formation Evaluation, Vol. 3, No. 2, p. 386-392.

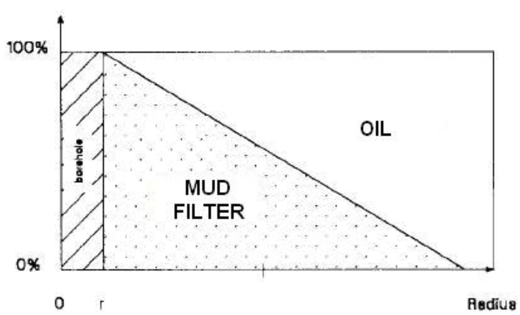

Figure 1. Ramp Model (modified from Singer & Barber, 1988).

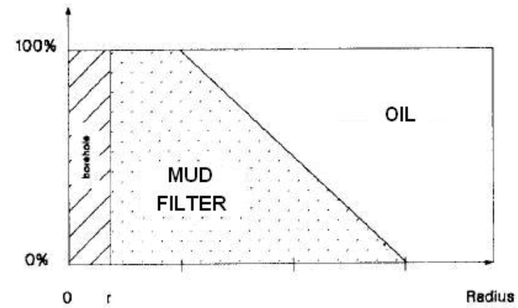

Figure 2. Slope Model (modified from Singer & Barber, 1988).

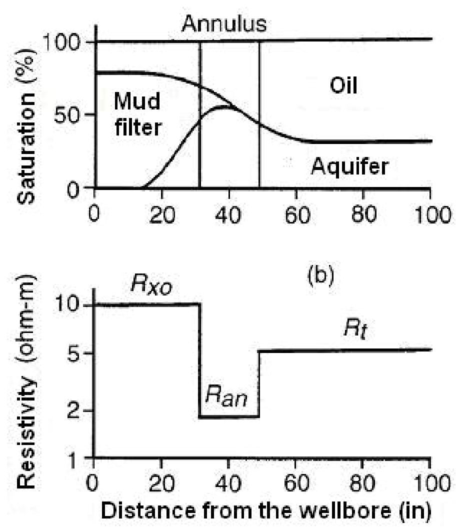

Figure 3. Annulus Model (modified from Anderson, 2002)

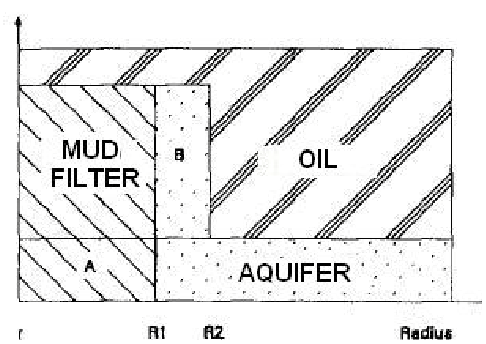

Figure 4. Annulus Model (modified from Singer e Barber, 1988)

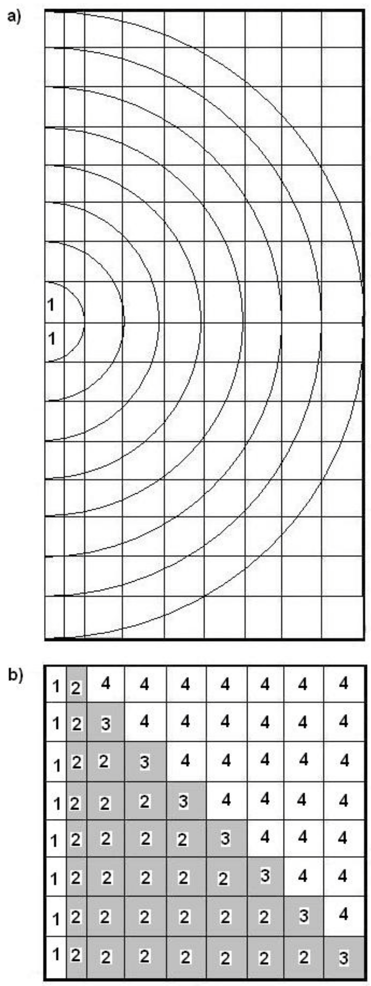

Figure 5. Half of the 3D ramp model a) Seen from the top. b) Transversal section.

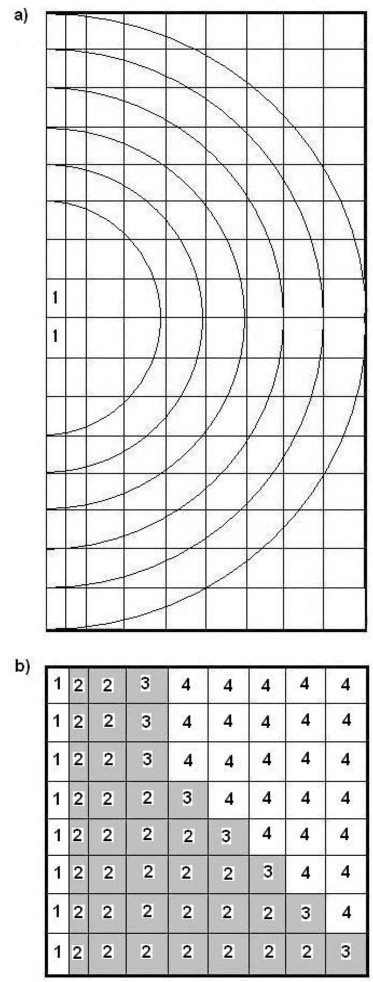

Figure 6. Half of the 3D slope model a) Seen from the top. b) Transversal section.

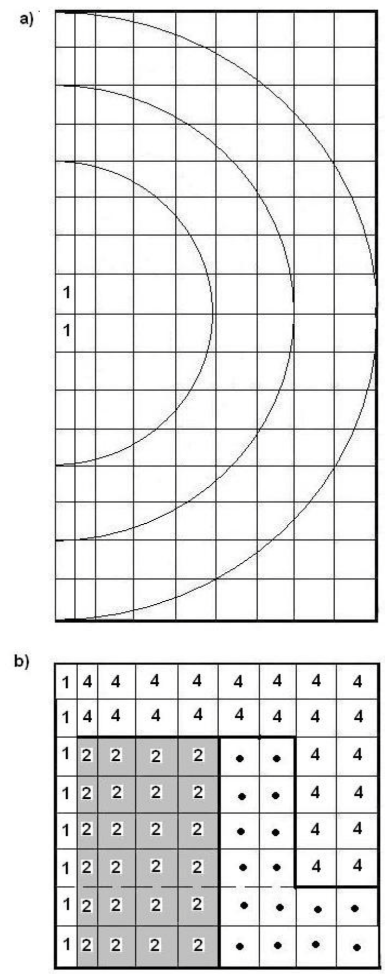

Figure 7. Half of the Annulus model a) Seen from the top. b) Transversal section.

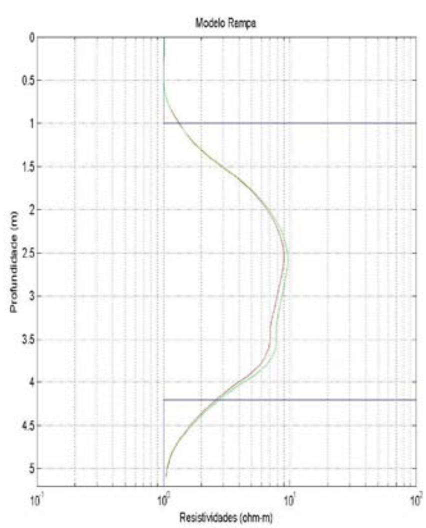

Figure 8. 6FF40 response for ramp model.

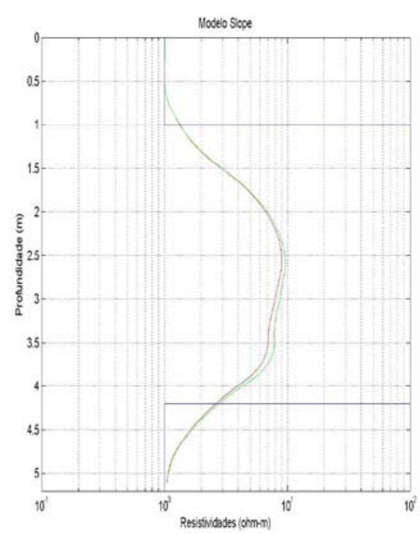

Figure 9. 6FF40 response for the slop model.

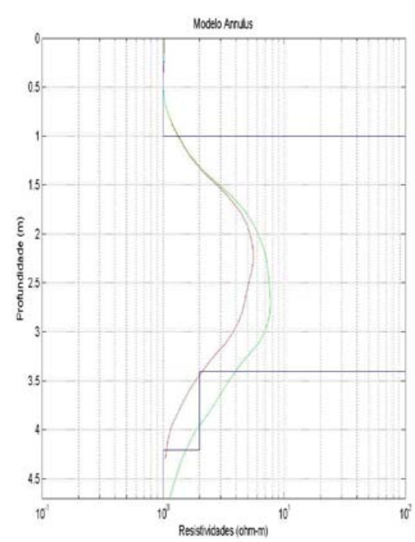

Figure 10. 6FF40 response for the annulus model.